JOURNAL OF PROPULSION AND POWER
Vol. 16, No. 1, January–February 2000

Very-Near-Field Plume Investigation of the Anode Layer Thruster

Matthew T. Domonkos,* Alec D. Gallimore,† Colleen M. Marrese,* and James M. Haas*
University of Michigan, Ann Arbor, Michigan 48109

The plasma properties of the very-near-field (10–50 mm) plume of the D55 anode layer thruster (TAL) were measured. The D55 is the 1.35-kW TAL counterpart to the SPT-100 and was made by the Central Scientific Research Institute of Machine Building of Kaliningrad, Russia. The thruster was tested in the 6 m diameter × 9 m long vacuum chamber at the University of Michigan's Plasmadynamics and Electric Propulsion Laboratory, and the diagnostic probes were positioned using a three-axis translation table system. Water-cooled Hall probes, a Faraday probe, emissive probes, and langmuir probes were used to examine the near-field plasma properties. Water-cooled Hall probes were employed to explore the effect of the closed-drift current on the radial magnetic field. The change in the magnetic field during thruster operation was found to be less than 5% over the region examined, which indicated that the Hall current was limited to several tens of amperes. Evidence also indicated that the closed-drift current extended between 5 and 10 mm downstream of the anode. Ion current density profiles showed that the annular beam focuses within 40 mm of the thruster exit plane. Plasma potential measurements indicated that ion acceleration occurred primarily within 10 mm of the anode. The highest electron temperature measured in this investigation occurred immediately downstream of the anode, and the temperature decreased with axial distance from the thruster. The low-energy electrons were confined to the high-density core of the plasma beam.

Nomenclature

A_n = differential area, mm^2
A_p = probe area, cm^2
B = magnetic field strength, G
E = ion energy, eV
e = charge of the electron, 1.6×10^{-19} C
I_c = control current for the Hall generator, A
I_e = electron current, A
I_i = ion saturation current, A
I_i' = dimensionless ion current
J_i = true ion current density, A/cm^2
$J_{i,FP}$ = measured ion current density, A/cm^2
k = Boltzmann's constant, 1.38×10^{-23} J/K
m_e = mass of the electron, 9.11×10^{-31} kg
m_i = ion mass, 2.18×10^{-25} kg
n_e = electron number density, cm^{-3}
r_p = langmuir probe radius, cm
T_e = electron temperature, eV
V = voltage, V
V_h = voltage output by the Hall generator, V
X = coordinate along thruster axis, mm
Y = coordinate direction of probe sweeps, mm
Z = coordinate denoting the elevation, mm
γ_e = secondary electron yield, electrons/ion
ε_0 = permittivity of free space, 8.85×10^{-12} F/m
λ_D = Debye length, cm

Introduction

THE D55 anode layer thruster (TAL) built by the Central Scientific Research Institute of Machine Building (TsNIIMASH) of Kaliningrad, Russia offers performance and a projected lifetime similar to that of the SPT-100 (Refs. 1 and 2). While this design is the result of years of empirically and theoretically derived improvements, current technology computer simulations have recently been employed to examine the physics of Hall thrusters without the need for analytic solutions of the governing equations.[3,4] By analyzing the physics with the greater detail afforded by numerical examination, the performance envelope of Hall thrusters can be explored and extended more effectively. This paper presents the results of the very near-field investigation along with a first-order calculation of some properties of the discharge.

The D55 TAL has a well-documented experimental heritage with Zharinov first proposing its design in the early 1960s.[5,6] Since the advent of Russian–American joint technological ventures in the early 1990s, the TAL has been under intensive experimental investigation in the United States.[2,7,8] The D55 is an alternative 1.35-kW thruster to the SPT-100 and T-100, with the benefits of increased thrust density and a potentially greater lifetime.[9] The work to date has focused on performance evaluation, examination of lifetime limitations, and far-field plume studies to assess spacecraft integration issues.[2,7,8] Garner et al.[2] conducted a 636-h test of the D55, which focused on performance mapping. Spacecraft integration issues were addressed in the work by Manzella and Sankovic,[7] which focused primarily on far-field plasma properties. In an effort to explain the erosion observed during the 636-h test, Marrese et al.[8] measured the magnetic field generated by the electromagnets alone, both within and upstream of the discharge region.

Although the vacuum magnetic field in Hall thrusters is expected to dominate the overall topography, the $\boldsymbol{E} \times \boldsymbol{B}$ closed drift of electrons may play a significant role in determining the field during thruster operation. Measurement of the magnetic field during thruster operation is one of the primary goals of the current investigation. Comparison of the field strengths from the magnets alone and during thruster operation enables estimation of the magnitude of the closed drift electron current and is of use for modeling efforts. To measure the magnetic field in the intense ion beam present in the near field of the thruster, water-cooled Hall probes were constructed that protect the delicate semiconducting Hall generator from the particle and radiative fluxes from the thruster. In addition to the magnetic field measurements, this investigation generates a map of plasma properties from 10 to 50 mm from the exit plane with greater radial resolution than previous work. Experiments performed by

Presented as Paper 97-3062 at the AIAA/ASME/SAE/ASEE 33rd Joint Propulsion Conference, Seattle, WA, 6–9 July 1997; received 9 October 1997; revision received 30 November 1998; accepted for publication 7 January 1999.

*Graduate Student Research Assistant, Plasmadynamics and Electric Propulsion Laboratory, Department of Aerospace Engineering, 1060 FXB Building, 1320 Beal Avenue. Student Member AIAA.

†Associate Professor, Plasmadynamics and Electric Propulsion Laboratory, Department of Aerospace Engineering, 3037 FXB Building, 1320 Beal Avenue. Senior Member AIAA.

TsNIIMASH have shown electron temperatures above 20 eV and plasma potentials of tens of volts within 15 mm of the exit plane and along the perimeter of the thruster. Previous work has illustrated some of the difficulties with examining the very near-field plasma generated by a Hall thruster.[10] Kim et al.[10] found electron temperatures and number densities of up to 8 eV and 3×10^{-12} cm^{-3} for the very-near-field plume of the SPT-100. These examinations provide a basis upon which to design electrostatic probes for this work.

This paper begins by describing the equipment used in this investigation. The experimental procedure is then described, followed by a presentation of the key results. The measurements of the magnetic field, ion current density, electron temperature, and number density are discussed, and a summary of the important results is presented.

Experimental Apparatus

All of the experiments were conducted in the Plasmadynamics and Electric Propulsion Laboratory (PEPL) 6 m diameter × 9 m long vacuum chamber, which is described in more detail elsewhere.[11] The facility is evacuated to high vacuum using six 0.81-m-diam oil diffusion pumps, for a total pumping speed of ~27,000 L/s on Xe, and the facility pressure was maintained at 8.3×10^{-3} Pa during testing. The charge exchange mean free path at this pressure is on the order of 1 m (Ref. 12), and, consequently, the plasma was treated as collisionless in the near field. A mass flow system controlled with micrometer valves at the vacuum feedthrough supplied 99.999% pure Xe to the thruster.

Thruster

The D55 TAL shown schematically in Fig. 1 was provided to PEPL by the Jet Propulsion Laboratory. The "55" indicates the mean diameter of the anode in millimeters. Figure 1 also defines the coordinate system used to refer to the data. The anode extends in an annulus to the exit plane of the thruster, which utilizes three outer electromagnets in contrast to the four in the SPT-100. The electromagnets were operated independently of the discharge at currents determined by TsNIIMASH. A LaB_6 hollow cathode designed by the Moscow Aviation Institute was used in these tests. The axis of the cathode was oriented at 45 deg to the centerline of the thruster. The cathode orifice was located 3 cm from the outer edge of the anode in both the positive X and Z directions. The cathode centerline fell along the $Y = 7$-mm plane of the thruster. The following summarizes the nominal D55 operating conditions during these tests: discharge voltage = 300 V, discharge current = 4.5 A, anode mass flow rate = 4.76 mg/s, cathode mass flow rate = 0.78 mg/s, cathode ground voltage = 13–15 V, and pressure = 8.3×10^{-3} Pa. The discharge was regulated using a resistance-capacitance filter with values of 25 Ω and 105 μF, respectively. Discharge was initiated at about 50 V and 3.0 A using a cathode igniter. After heating for several minutes, the thruster was shut off and immediately restarted at high voltage (>200 V on the discharge) to mitigate power-supply difficulties associated with the transition of the thruster from low-voltage (<100 V) to high-voltage operation. The thruster was mounted on a post connected to the same plate as the probe-positioning system. This configuration prevented misalignment of the diagnostic probes due to warping of the chamber under vacuum.

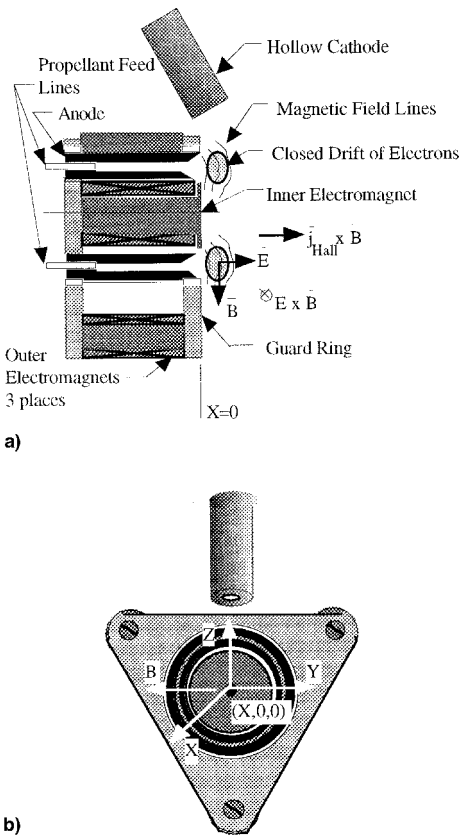

Fig. 1 Schematic of the D55 anode layer thruster: a) side section and b) front views.

Positioning System

A three-axis positioning system was used to map the vacuum magnetic field of the D55 in the very near field. To minimize the perturbation of the plasma plume, the Z-translation stage was omitted for all measurements taken during the thruster discharge. Consequently, the plasma parameters and the magnetic field in the plasma were measured in the X–Y plane only. All reported positions are accurate to within 2 mm.

Using the positioning system, data were gathered in sweeps along the Y axis for the Hall and Faraday probes, as illustrated in Fig. 2. A single sweep contained several hundred samples along a line of constant X and Z, and, consequently, these data are reported here as continuous curves for clarity in the plots. Vacuum magnetic field data sweeps were gathered at discrete values of X and Z, ranging from 5 to 50 mm and −60 to 40 mm, respectively. To report radial magnetic field data, the Y and Z components, measured separately with a transverse Hall probe, were used to calculate the radial field at discrete points in a 21 × 100 matrix in a plane of constant X. Ion current densities were measured only along lines of constant X and $Z = 0$ in the X–Y plane. Both the magnetic field and the ion current density measurements were recorded on a digital oscilloscope to ensure that the sampling rate was sufficient to capture data every 0.5 mm of travel. In contrast, measurements made with the langmuir and emissive probes were taken by positioning the probe at a single point in the plume, downloading the data from an oscilloscope to a

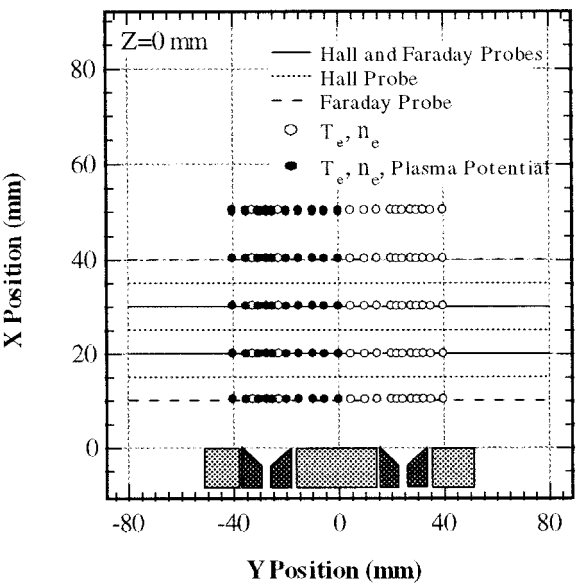

Fig. 2 Data sampling in the X–Y plane.

computer, then moving the probe out of the plume. These sampling locations are shown in Fig. 2 as well.

Hall Probes

Figure 3 shows the water-cooled Hall probes used to measure the magnetic fields of both the electromagnets and the thruster during operation. Magnetic fields deflect the constant current I_c supplied to the Hall probe, which results in the generation of an electric field in the direction mutually perpendicular to the constant current and the magnetic field. The induced voltage V_H is proportional to the applied magnetic field. Because the Hall generator is a semiconductor device, the operating temperature must remain below 100°C. F. W. Bell BH-208 axial and BH-209 transverse Hall generators comprised the sensor elements on two separate probe assemblies. The generators were mounted to nonmagnetic stainless-steel water-cooling tubes using ceramic cement. This configuration provided a thermal conduction path from the Hall probe to the cooling tubes and a radiation shield of ceramic cement. In addition to these thermal management systems, a Pyrex® flux shield insulated the Hall probe elements against heat deposition by plasma bombardment. A refrigerated recirculator maintained an inlet water temperature of 7°C. A small type K thermocouple was used to monitor the temperature of the Hall probe so that thermal drift of the transducer output was accounted for in the analysis of the signal. If the temperature drifted beyond 24°C, the probe was left out of the plume for an extended period to reduce the temperature.

Because the output of the Hall probe was expected to be on the order of hundreds of microvolts, the signal was amplified within 1 m of the Hall generator by a 1000-gain Analog Devices 524AD precision instrumentation amplifier. The output of the amplifier was recorded with a digital oscilloscope in high-resolution acquisition mode. The bandwidth of the oscilloscope was adjustable to 500 MHz. A Lambda LPD-422A-PM power supply provided the constant current I_c to drive the probes.

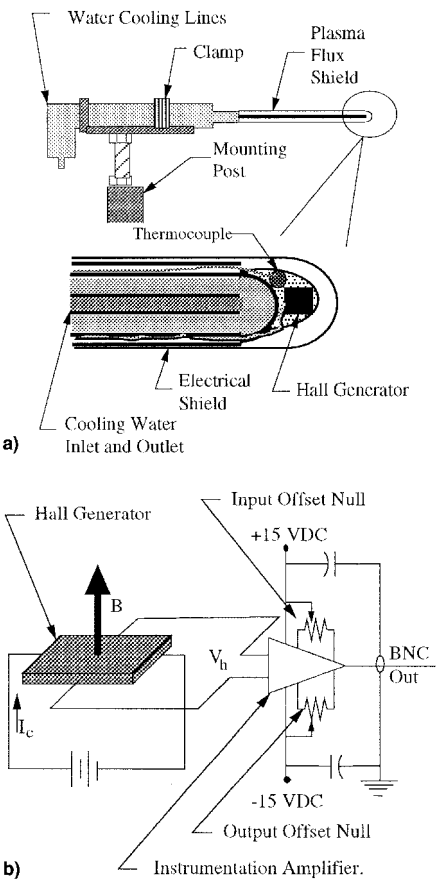

Fig. 3 Schematic of the water-cooled Hall probes used in the D55 tests: a) mechanical diagram and b) electrical schematic.

The Hall probes were calibrated against a National Institute of Standards and Technology traceable Walker Scientific MG-5DAR Gaussmeter. Figure 4a shows the calibration of the transverse probe with respect to the Gaussmeter, and Fig. 4b shows that a strong axial electric field had a negligible effect on the sensitivity of the generator. Examination of the calibration in Fig. 4a indicates an accuracy of 1–2 G for the Hall generator. The applied electric field of 15,000 V/m was estimated to be the maximum field strength in the anode layer thruster. The nonzero voltage at zero magnetic field was the result of an imperfect Hall generator and constituted an offset. The offset may be adjusted using the potentiometers in Fig. 3b. Figure 4b shows a hysteresis loop because the cores of the Helmholtz coils were slightly ferromagnetic and the applied current would induce residual magnetism in the cores. Consequently, the order in which the data were taken was identical for all calibrations to ensure accuracy. An electromagnet was positioned inside the vacuum chamber to provide in situ calibration of the probes.

The Hall probes were used to measure the magnetic field generated by the thruster both with and without a discharge. During thruster operation, the aforementioned positioning system was used to move the Hall probes through the very-near-field plume or to the calibration electromagnet. Based on calibrations, sweep-to-sweep variations in the field strength, and conversion of data taken in transverse sweeps to radial information, the diagnostic was estimated to be accurate to within ±5 G. This number reflects possible misalignment of the probe with respect to the thruster axis and vibrations experienced by the probe during its traverse through the plume. The thermal design of the probes adequately protects the Hall generator from the heat flux of the thruster for short periods. To minimize the energy deposition to the probe, the positioning system was operated at sweep speeds of 10–20 cm/s. Consequently, improving the overall accuracy would involve a redesign of the support structure to mitigate vibration at the speeds necessary to protect the probe.

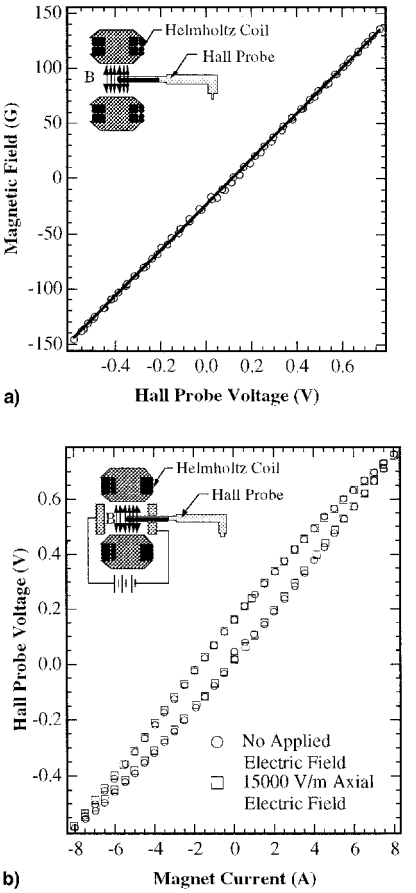

Fig. 4 Calibration of the Hall probe: a) Hall probe calibration curve and b) evaluation of the effect of a strong electric field on Hall probe response.

Electrostatic Probes

A planar Faraday probe consisting of a 2.4-mm-diam tungsten rod sheathed in an alumina tube was used to measure the ion current density. The tungsten rod was insulated from the plasma except for the end that collected the ion current. A guard ring was omitted for simplicity. The probe diameter was much greater than the Debye lengths, which ranged from 4×10^{-3} to 3×10^{-2} mm, thereby limiting the impact on the effective collection area of the probe to approximately 5%. The probe was biased −70 V with respect to ground, which was deemed sufficient to repel the electron current because further negative increases resulted in a negligible increase in ion current. Secondary electron emission by Xe bombardment of the tungsten probe was taken into account using Eq. (1):

$$J_i = J_{i,FP} - \gamma(\langle E \rangle) J_{i,FP} \tag{1}$$

where γ is the secondary emission coefficient evaluated at the average ion energy. Because the yield for Xe ions bombarding tungsten is nearly constant over the range of possible ion energies, a value of 0.018 was used in the reported current densities.[13] Hagstrum[13] omitted the accuracy of the secondary emission coefficient. Current was determined by measuring the voltage drop across a 92-Ω shunt resistor. Based on the errors in the measured current and the estimated sheath size, the error in the ion current densities reported here was ~5.2%.

Cylindrical langmuir probes were used to measure the electron number density and temperature. The probes consisted of 0.127 mm diameter × 5 mm long tungsten wire encased in an alumina tube housing. The probe was biased with respect to ground using a bipolar power supply, and the ground-to-cathode potential was monitored to facilitate data presentation. For the purposes of analysis, the ions and electrons were assumed to form Maxwellian distributions. The effect of the magnetic field will be to impede the flow of electrons to the probe, which results in a reduction in the collected current and the apparent electron number density. At all locations examined in this work, the electron and ion Larmor radii were larger than the probe radius, and the effects of the magnetic field on the probe response were neglected.[14] Consequently, the electron temperature was calculated using Eq. (2):

$$T_e = \frac{e}{k}\left\{\frac{\mathrm{d}[\ell n(I_e)]}{\mathrm{d}V}\right\}^{-1} \tag{2}$$

where I_e is the electron current to the probe, and the derivative is evaluated as the slope of $\ell n(I_e)$ near the floating potential. The plasma potential was determined by the inflection-point method where the peak of the first derivative of the probe current with respect to voltage defines the plasma potential. The electron number density was evaluated using the method described by Sonin[15] for the assumption that the electron temperature is much greater than the ion temperature. This analysis, based on the work by Laframboise,[16] allows calculation of the product of the dimensionless ion current with the square of the ratio of probe radius to Debye length using Eq. (3)[15,17]:

$$I_i'\left(\frac{r_p}{\lambda_D}\right)^2 = \frac{r_p^2}{\varepsilon_0}\left(\frac{2\pi m_i}{e}\right)^{0.5}\left(\frac{e}{kT_e}\right)^{1.5}\frac{I_i}{A_p} \tag{3}$$

This quantity, which is calculated using directly measured quantities, is used to determine the dimensionless ion current independent of the number density. In the cold ion approximation, the relation between Eq. (3) and the dimensionless ion current is given in a plot in Sonin.[15] Once the dimensionless ion current has been determined, the electron number density can be calculated from Eq. (3). This theory accounts for the various ratios of probe radius to Debye length encountered in this investigation.

The emissive probes were constructed from 0.064-mm-diam tungsten wire with a 4-mm-long single loop to measure the local plasma potential. The loop was connected electrically by two 0.23-mm-diam tungsten wires and two much larger copper wires, which were mounted within a two-hole ceramic insulator. For electrical and mechanical shielding, the assembly was encased in a 2.6-mm-diam, thin-wall stainless-steel jacket. The spatial resolution was limited axially by the filament length of 2.5 mm and laterally by the support structure width of 1.5 mm.

The filament was heated to emission with a 60-Hz half-wave rectified heating current. The probe bias voltage with respect to ground was swept at 500 Hz with measurements taken during the off phase of the heater when the filament had a unipotential surface and a correction for longitudinal potential drop across the probe was unnecessary. The inflection point method with the current–voltage trace of a hot electron emitting filament was used to determine the plasma potential.[18]

Results and Discussion

Magnetic Field

Because of the proprietary nature of the magnetic field data, the values reported in this paper have been normalized to the maximum vacuum axial or radial field strength 5 mm from the exit plane, $X = 5$ mm. The normalized errors were ±0.022 and ±0.027 in the axial and radial magnetic fields, respectively. Measurements during thruster operation were limited to within 15 mm axially from the exit plane (see Fig. 2). Attempts to probe closer resulted in perturbations in the operation of the D55. The tip of the probe extended 5 mm beyond the Hall generator, and the presence of a cool insulating surface at this distance caused the thruster current to rise to as much as 8 A while the assembly was directly downstream of the anode ($\sim Y = \pm 27.5$ mm). It is believed that due to this particular perturbation of the thruster, $X = 5$ mm represents the axial extent of the closed drift of electrons in the D55.

A comparison of the magnetic field at $X = 15$ mm, generated by both the electromagnets alone and the operating thruster, is depicted in Fig. 5. Overall, the field strength at $Y = \pm 25$ mm diminished by less than 7 G; this was established by comparing the differences from both $Y = +25$ and -25 mm and using the fraction that was beyond the uncertainty of the measurement. At least 95% of the vacuum field strength generated by the electromagnets alone remained during thruster operation. This limited the Hall current to several tens of amperes, assuming it was the primary contributor to the change in the magnetic field. The small change also indicates that vacuum field measurements are within 5% of the discharge values. For applications where this error is acceptable, the magnetic field during thruster operation can be approximated by the vacuum field measurement. The benefit of this result is that a Gaussmeter or a simplified Hall probe is sufficient to map the magnetic field, and these devices offer improved capability for resolution compared with water-cooled Hall probes with their extensive thermal protection.

As a result of the small difference between the vacuum and discharge magnetic fields, Figs. 6 and 7 present contour maps of the axial X and radial vacuum magnetic fields 5 mm from the exit plane, $X = 5$ mm, obtained with the Gaussmeter. These maps show the geometry of the thruster for reference, and the scale is only approximate. The inner electromagnet generates the largest fraction of the

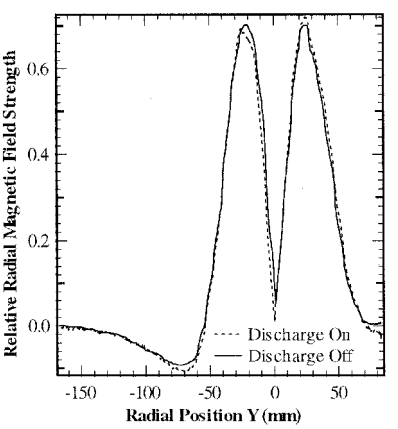

Fig. 5 Comparison of the vacuum field generated by the electromagnets and the field generated during thruster operation, $X = 15$ mm.

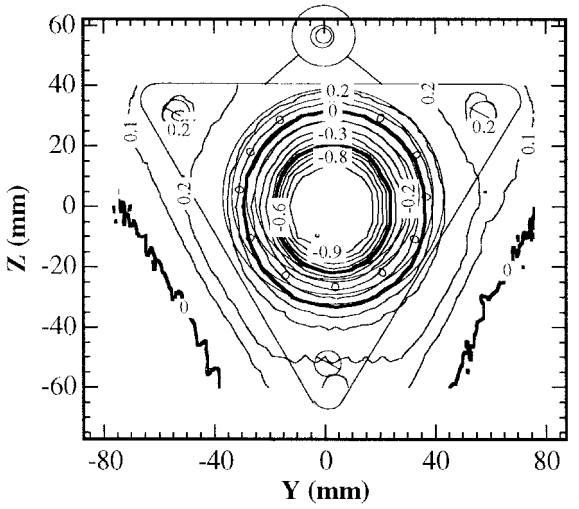

Fig. 6 Axial magnetic field contours 5 mm from the exit plane of the D55. Positive values indicate a field directed toward the thruster.

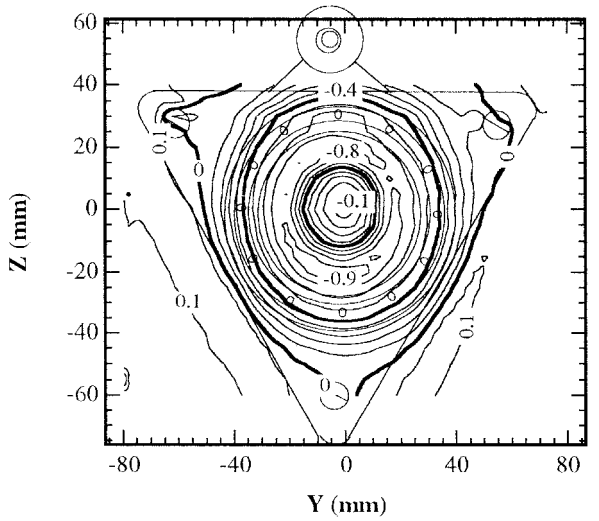

Fig. 7 Radial magnetic field contours 5 mm from the exit plane of the D55. Positive values indicate a field directed toward the thruster axis.

magnetic field. The axial contours show a high degree of symmetry about the X axis, although the outer electromagnet at 150 deg to the Y axis appears to be slightly stronger than the one at 30 deg. Given that the axial magnetic field was measured directly and is free of the numerical errors associated with calculating the radial field, this small perturbation is beyond the limits of error in the measurement. The radial contour map shows a similar asymmetry. The strongest radial fields were observed in the third quadrant of the $Y-Z$ plane. This type of asymmetry suggests that the outer electromagnet at 30 deg is slightly weaker than its two counterparts. A misalignment of the probe system with respect to the thruster would result in one side of the thruster appearing to be stronger than the other; however, the indicators were more localized, suggesting a truly asymmetric magnetic field. It should also be noted that in Fig. 7, the radial field map shows a numerical defect in the range of $Z = 35$ mm. The contours change abruptly in this region, and the phenomenon was absent in the axial field contours.

The fields downstream of $X = 5$ mm are expected to share the structure of the contours shown in Figs. 6 and 7 with a diminished scale. The axial variation of the radial field presented in Fig. 8 shows the expected decay. These data were taken during thruster operation. This information was used to calculate the Larmor radius to establish the validity of neglecting magnetic field effects on electrostatic probe results.

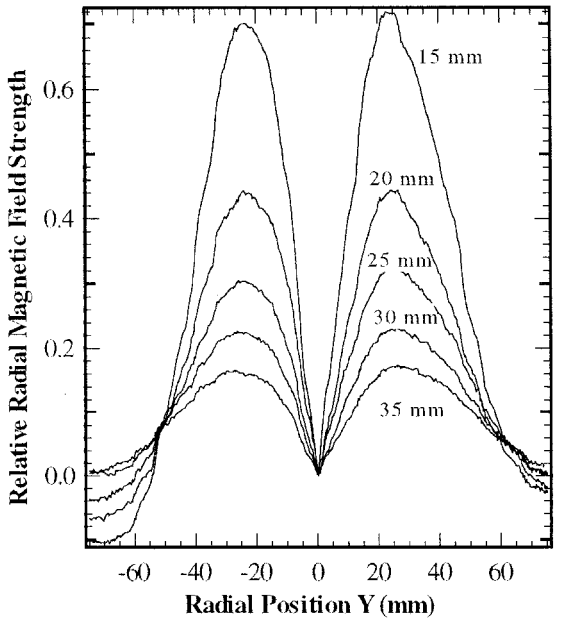

Fig. 8 Axial variation of the radial magnetic field. The numbers on the plot indicate the position X.

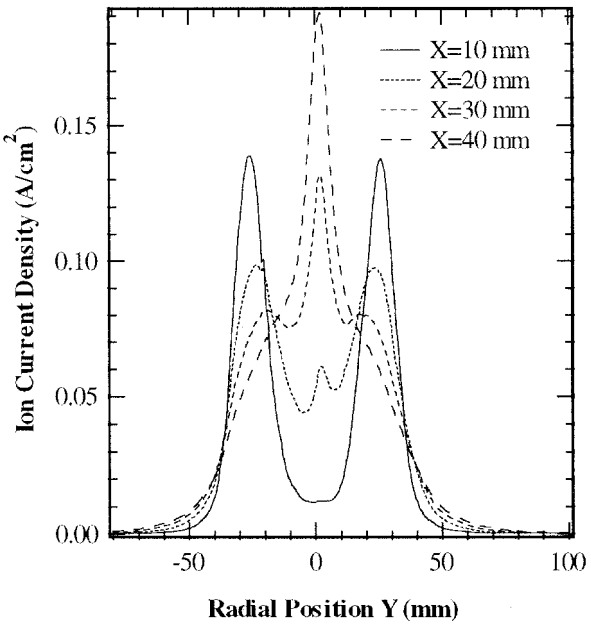

Fig. 9 Ion current density sweeps between 10 and 40 mm axially.

Ion Current Density

Figure 9 depicts the variation of the ion current with axial distance from the thruster. The ion beam begins as an annulus, but within 40 mm of the discharge chamber coalesces to a single axisymmetric jet. Compared with a similar study of the SPT-100 (Ref. 10), the plume of the D55 focuses in a much shorter distance. The integrated ion currents are presented in Table 1. These currents were computed by summing the product of the current density at a position (X, Y, 0) and the differential area

$$A_n = \pi \left[\left(\frac{Y_{n+1} + Y_n}{2} \right)^2 - \left(\frac{Y_n + Y_{n-1}}{2} \right)^2 \right] \qquad (4)$$

where n denotes the nth measurement of the ion current density. Given the symmetry in the ion current density measurements, only data at positive values of Y were used. At all axial locations, the

Table 1 Calculated ion current based on the ion current density measurements

Axial (X) location, mm	Integrated ion current, A
10	3.85
20	3.54
30	3.63
40	3.59

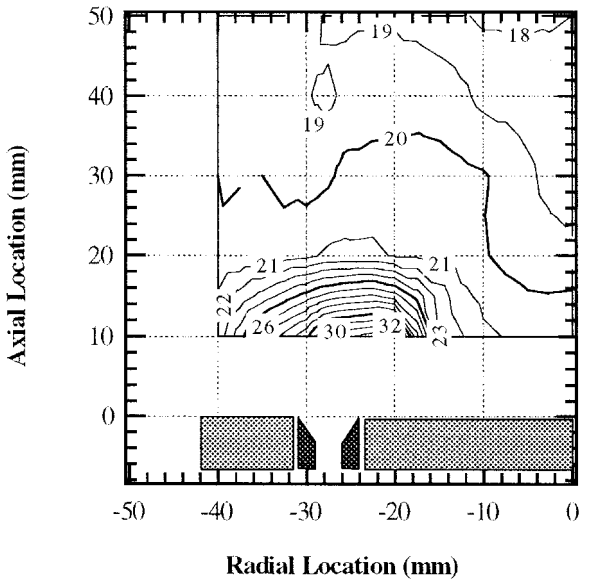

Fig. 10 Plasma potentials with respect to cathode in the very-near-field of the D55.

ion current was lower than the discharge current. This was expected because ions born near the anode and in the acceleration region carry a fraction of the discharge current, whereas electrons diffusing through the closed drift to the anode provide the remaining current. It should also be noted that the probe was always parallel to the axis of the thruster. At high angles between the flow and the probe face, the projected ion collection area is less than the value used in the calculations. Consequently, the ion current density is underestimated at large positive and negative values of Y.

Plasma Potential

Both langmuir and emissive probes were used to measure the plasma potential. A contour plot of the plasma potential determined with the langmuir probe with respect to the cathode is shown in Fig. 10. The emissive probe data corroborated the langmuir probe data, although it was consistently 1–2 V lower. The error in the langmuir probe measurements was determined by examining the width of the peak in the derivative of the probe current. The uncertainty in the langmuir probe inflection point yielded an error of ±1 V for the data between $X = 20$ and 50 mm. The derivative of the current was considerably less smooth at $X = 10$ mm than at other locations, and, consequently, the error on these measurements was estimated to be ±3 V. The contour plot clearly shows the downstream extent of the acceleration region. The ions have essentially completed their acceleration 20 mm downstream of the thruster, although the greatest fraction of the acceleration occurs within the first 10 mm. The plot illustrates not only the axial acceleration, but also the tendency of the plasma potential to focus the ion beam as evidenced by the reduced plasma potentials near the axis. Attempts to probe closer than 10 mm were unsuccessful because the probe interfered with the thruster operation. Plasma potentials were measured through $Y = 40$ mm at $X = 50$ mm, and were found to be symmetric within the accuracy claimed.

Because the anode of the D55 extends to its exit plane, the closed drift of electrons and the acceleration region necessarily extend beyond the exit plane, as shown schematically in Fig. 1. All efforts to measure properties within 10 mm axially of the anode resulted in an increase in the discharge current of several amperes. A probe in the closed-drift of electrons will either short the plasma across the magnetic field lines or ablate, increasing the local number density and conductivity. Either effect results in a reduction of the impedance of the plasma and an increase in the current at a constant voltage. Both the plasma potential data presented in Fig. 10 and the anecdotal evidence when probing close to the thruster indicate that the ions are accelerated to around 270 V within the first 10 mm.

Electron Temperature and Number Density

The radial variation of the electron temperature is presented in Fig. 11. Error analysis was based on the variation in the curve fits to the natural logarithm of the electron current. It was assumed that in the very near field, the flow vector was parallel with the axis of the thruster, and, thus, the probe alignment with the axis minimized the error due to misalignment.[15] This resulted in a typical accuracy of ~±15%. At $X = 10$ mm, the electron temperature peaked at 10.5 eV, which is slightly higher than reported values for other Hall thrusters.[10,19] The profiles plateau in the periphery of the beam and dip in the center. The slight misalignment of the cathode orifice at $Y = 7$ mm accounts for the lower electron temperatures observed at radial positions where $Y > 0$ mm. As the electrons move axially, the electron temperature decreases and the magnitude of the radial temperature variation diminishes in the very near field. Based on the ion current density measurements, the beam focuses to a single column within 40 mm of the exit plane, and the electrons must follow the ions to maintain quasineutrality in the beam. The low-energy electrons follow the ions in the beam, and, consequently, the plasma at radial positions outside of the beam is populated by a greater fraction of high-energy electrons than along the axis. This manifests itself in peak electron temperatures at some radial distance from the core of the beam, which is effectively the trend illustrated in Fig. 11.

Figure 12 shows the axial variation of the electron number density. These data have a predicted accuracy of ±60% based on the calculated and measured quantities in Eq. (3). As expected, the profile at $X = 10$ mm had a peak in the region of the discharge chamber. The peak moved to the thruster axis within 20 mm of the exit plane. This structure was similar to that observed with the ion current density. First-order calculations of the ion number density based on the local ion current density and a 280 V accelerating potential resulted in comparable number densities within the 60% accuracy claimed for the electron number density measurements.

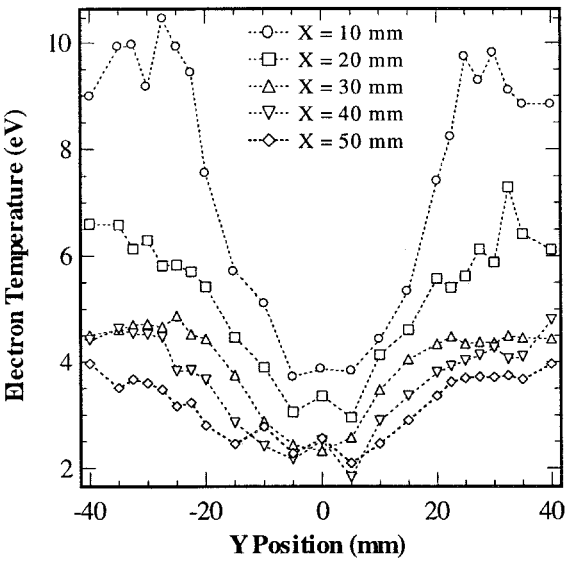

Fig. 11 Electron temperatures in the very-near-field of the D55.

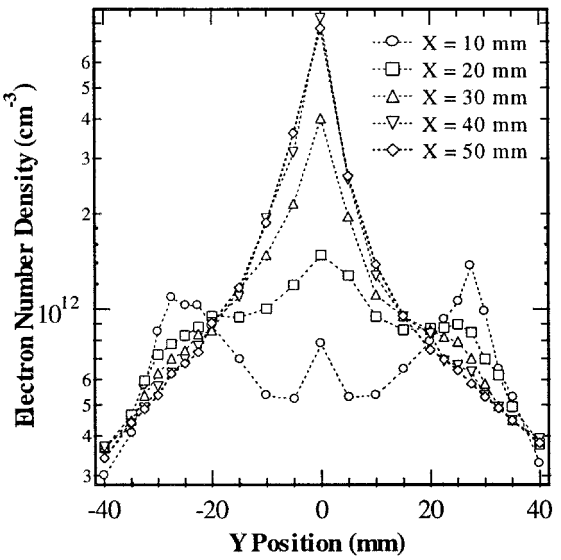

Fig. 12 Electron number densities in the very-near-field of the D55.

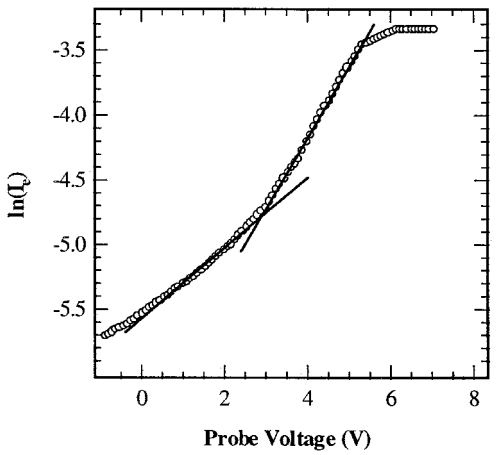

Fig. 13 Non-Maxwellian character of the electron current.

Probe Considerations

The analysis of the langmuir probe data assumes Maxwellian distributions of both electron and ion energies. Research by Baranov et al.[20] has shown the existence of a high-energy tail in the electron energy distribution function. This result is supported by the shallow curvature observed in the plots of the natural logarithm of the electron current vs voltage as seen in Fig. 13; a Maxwellian population generates an entirely linear plot in the region of the floating potential. In every case, two different electron temperatures could be calculated in this part of the probe characteristic. This is evidence of a non-Maxwellian electron population, possibly composed of two Maxwellian populations at different temperatures. To accurately assess the electron energy, the distribution function must be evaluated. This is beyond the scope of the present investigation.

Conclusions

An extensive probe-based investigation of the very-near-field plume and magnetic field of the D55 was conducted. Water-cooled Hall probes were used to measure the magnetic field generated by the electromagnets alone and during thruster operation. The results showed that the field present during thruster operation was ~95% of the strength of the vacuum field. Consequently, only the vacuum field must be measured if this small inaccuracy can be tolerated. By assuming that the closed-drift current caused all of the 5% reduction in the magnetic field strength, the Hall current was estimated to be several tens of amperes. The inadvertent disruption of the discharge by the tip of the Hall probe indicated that the drift current extends at least 5 mm from the anode. Ion current densities were also measured, and the annular beam present at the discharge chamber coalesces into a single peaked profile within 40 mm of the exit plane of the thruster. The plasma potential measurements provided quantitative evidence that most of the acceleration of the ions occurs within 10 mm of the anode. Electron temperature and number density were measured using cylindrical langmuir probes. Low-temperature electrons populated the core of the ion beam, and the high-energy electrons were more prevalent far from the thruster axis. Conversely, the number density profiles were very similar to the ion current density curves, with a central peak becoming prominent in the radial profile 30 mm from the exit plane of the thruster.

Evaluation of the Debye lengths and Larmor radii showed that the analysis performed in this work was within the bounds of validity for the theory. The character of the electron temperature measurements suggested a non-Maxwellian plasma, and future work should address the extent to which the Maxwellian plasma assumption affects the results presented here.

Acknowledgments

The NumerEx Corporation of Albuquerque, New Mexico was under contract with the Jet Propulsion Laboratory to develop a magnetohydrodynamics model of the operation of the D55. This research was supported by a research grant from NumerEx Corporation of Albuquerque, New Mexico, and the Jet Propulsion Laboratory. Michael Frese was the Contract Monitor. The D55 was provided by the Jet Propulsion Laboratory. The authors thank Alexander Semenkin and Sergei Tverdokhlebov of TsNIIMASH for their generous and patient support in operating the D55. Additional thanks go to Sergei Khartov of the Moscow Aviation Institute for the use of the cathode, and to Sven G. Bilén for his assistance with the Hall probe diagnostic.

References

[1]Sankovic, J. M., Hamley, J. A., and Haag, T. W., "Performance Evaluation of the Russian SPT-100 Thruster at NASA LeRC," *Proceedings of the 23rd International Electric Propulsion Conference*, Vol. 2, Electric Rocket Propulsion Society, Columbus, OH, 1993, pp. 855–882.

[2]Garner, C. E., Brophy, J. R., Polk, J. E., Semenkin, S., Garkusha, V., Tverdokhlebov, S., and Marrese, C. M., "Experimental Evaluation of the Russian Anode Layer Thruster," 3rd Russian-German Conf. on Electric Propulsion Engines and Their Technical Applications, Stuttgart, Germany, July 1994.

[3]Oh, D., and Hastings, D., "Axisymmetric PIC-DSMC Simulations of SPT Plumes," *24th International Electric Propulsion Conference*, Vol. 2, The U.S. Air Force European Office of Aerospace Research and Development, Stuttgart, Germany, 1995, pp. 1105–1114.

[4]Rhee, M. S., and Lewis, M. J., "Numerical Simulation of Stationary Plasma Thruster Exhaust Plume," AIAA Paper 95-2928, July 1995.

[5]Kervalishvili, N. A., and Zharinov, A. V., "Characteristics of a Low-Pressure Discharge in a Transverse Magnetic Field," *Soviet Physics—Technical Physics*, Vol. 10, No. 12, 1966, pp. 1682–1687.

[6]Zharinov, A. V., and Popov, Y. S., "Acceleration of Plasma by a Closed Hall Current," *Soviet Physics—Technical Physics*, Vol. 12, No. 2, 1967, pp. 208–211.

[7]Manzella, D. M., and Sankovic, J. M., "Hall Thruster Ion Beam Characterization," AIAA Paper 95-2927, July 1995.

[8]Marrese, C. M., Polk, J. E., King, L. B., Gallimore, A. D., Semenkin, S., Garkusha, V., and Tverdokhlebov, S., "Analysis of Anode Layer Thruster Guard Ring Erosion," *24th International Electric Propulsion Conference* (Moscow, Russia), Vol. 2, The U.S. Air Force European Office of Aerospace Research and Development, Stuttgart, Germany, 1995, pp. 1326–1333 (Paper 95-196).

[9]Garkusha, V., Podgornov, V. A., Semenkin, A. V., and Chislov, G. O., "Erosion Measurements at the 260-Hour Test of the Thruster with External Anode Layer," 3rd Russian-German Conf. on Electric Propulsion Engines and Their Technical Applications, Stuttgart, Germany, July 1994.

[10]Kim, S. W., Foster, J. E., and Gallimore, A. D., "Very-Near-Field Plume Study of a 1.35 kW SPT-100," AIAA Paper 96-2972, July 1996.

[11]Gallimore, A. D., Kim, S.-W., Foster, J. E., King, L. B., and Gulczinski, F. S., "Near- and Far-Field Plume Studies of a One-Kilowatt Arcjet," *Journal of Propulsion and Power*, Vol. 12, No. 1, 1996, pp. 105–111.

[12]King, L. B., "Transport-Property and Mass Spectral Measurements in the Plasma Exhaust Plume of a Hall-Effect Space Propulsion System," Ph.D.

Dissertation, Aerospace Engineering Dept., Univ. of Michigan, Ann Arbor, MI, 1998.

[13]Hagstrum, H. D., "Auger Ejection of Electrons from Tungsten by Noble Gas Ions," *Physical Review*, Vol. 96, No. 2, 1954, pp. 325–335.

[14]Hutchinson, I. H., *Principles of Plasma Diagnostics*, Cambridge Univ. Press, New York, 1992.

[15]Sonin, A. A., "Free-Molecule Langmuir Probe and Its Use in Flowfield Studies," *AIAA Journal*, Vol. 4, No. 9, 1966, pp. 1588–1596.

[16]Laframboise, J. G., "Theory of Spherical and Cylindrical Langmuir Probes in a Collisionless, Maxwellian Plasma at Rest," Univ. of Toronto Inst. for Aerospace Studies, Rept. 100, Toronto, ON, Canada, June 1966.

[17]Bullock, S. R., and Myers, R. M., "An Investigation of Magnetic Field Effects on Plume Density and Temperature Profiles of an Applied-Field MPD Thruster," *Proceedings of the 23rd International Electric Propulsion Conference*, Vol. 2, Electric Rocket Propulsion Society, Columbus, OH, 1993, pp. 1292–1307.

[18]Smith, J. R., Hershkowitz, N., and Coakley, P., "Inflection-Point Method of Interpreting Emissive Probe Characteristics," *Review of Scientific Instruments*, Vol. 50, No. 2, 1979, pp. 210–218.

[19]Bishaev, A. M., and Kim, V., "Local Plasma Properties in a Hall-Current Accelerator with an Extended Acceleration Zone," *Soviet Physics—Technical Physics*, Vol. 23, No. 9, 1978, pp. 1055–1057.

[20]Baranov, V. I., Nazarenko, Y. S., Petrosov, V. A., Vasin, A. I., and Yashnov, Y. M., "Electron Distribution Function in Accelerator with Closed Electron Drift," *Proceedings of the 24th International Electric Propulsion Conference*, Vol. 1, The U.S. Air Force European Office of Aerospace Research and Development, Stuttgart, Germany, 1995, pp. 440–444.